Available online at www.sciencedirect.com

ScienceDirect

Procedia Engineering 132 (2015) 561 – 568

Procedia Engineering

www.elsevier.com/locate/procedia

The Manufacturing Engineering Society International Conference, MESIC 2015

# Design analysis of a machined part in a single step to replace a structural component assembled through non-destructive testing and FEA

I. Mendoza-Muñoz[a,*], V. Nuño-Moreno[a], A. González-Ángeles[a], M. Siqueiros-Hernández[b], L. Moreno-Ahedo[a], M. Montoya-Reyes[a]

[a]*Faculty of Engineering, Autonomous University of Baja California (UABC). Blvd. Benito Juarez s/n, Col. Ex Ejido Coahuila, Mexicali B.C., 21900, México.*

[b]*Engineering and Technology Center, Autonomous University of Baja California (UABC). Blvd. Universitario #1000, Unidad Valle de las Palmas, Tijuana B.C., México.*

**Abstract**

In this study, a design analysis was performed through non-destructive test by rectangular rosette and uniaxial strain gages with FEA, between a structural aerospace assembled component of aluminium and a proposal part machined in one step with the same geometric characteristics. The analysis showed that the proposal part machined in one step has a trend to obtain less strain (0.5156mε@46.44N rectangular rosette strain gage, 0.4796 FEA) than the assembled component (0.7012mε@46.44N rectangular rosette strain gage, 0.7793 FEA). These findings indicate that the proposal part is a structural element with greater structural stiffness in comparison to the assembled component.


Peer-review under responsibility of the Scientific Committee of MESIC 2015

*Keywords:* ANSYS; FEA; Strain Gages; DFMA; Aerospace Parts.

## 1. Introduction

Variety in product design exists regardless of the structural complexity of the product, which might be a simple light bulb or a complex automobile or airplane. This variety propagates through the various assembly levels of each

* Corresponding author. Tel.: +52-686-5636-4270 ext. 1370; fax: +52-686-5636-4270 ext. 1305.
*E-mail address:* ismael.mendoza@uabc.edu.mx


Peer-review under responsibility of the Scientific Committee of MESIC 2015
doi:10.1016/j.proeng.2015.12.533

product variant, into subassemblies, modules, components and parts. Proliferation of product variation and the consequential variety levels across products structure affect all related manufacturing activities; specifically designing and processing in manufacturing [1].

In a large manufacturing company, new ideas have been generated by product engineers and designers mutually in product design stage by analyzing various aspects of the design, investigating capabilities and limitations of the production system. Currently, conventional CAD/CAM systems are commonly used for swift design and revision of products. However, in those systems product design is based on ordinary geometric modelling method. On the other hand, Design For Manufacture (DFM), Design For Assembly (DFA) have been used widely for finding optimum cost, significant improvement in quality, reliability and superior product design [2].

Design For Manufacture (DFM) is a systematic procedure to maximize the use of manufacturing processes in the design of components and Design For Assembly (DFA) is a systematic procedure to maximize the use of components in the design of a product. To be effective in product design, the procedures are often combined as Design For Manufacture and Assembly (DFMA). DFMA is a systematic procedure for analyzing proposed designs from the perspective of assembly processes. To obtain the maximum benefit from DFMA, the procedure is applied as early as possible in the design process and used within a concurrent engineering teamwork environment [3].

Joining and assembly can account for up to 30% of a product's total manufacturing cost and up to 50% of its total manufacturing time. If that does not sufficiently underline the importance, then consider that joining can impact considerably on product performance, for example, by introducing stress concentrations or by modifying the microstructure and properties (sometimes catastrophically: many failure analyses trace their origins back to joints). Assembly may come toward the end of product manufacture, but it is potentially an expensive mistake to leave it to the end of the design process—if only at the basic level of ensuring access to the joining equipment on a production line. Joining and assembly problems have been the Achilles' heel of many designs and products [4].

The F-22 program incorporated DFMA practices such as ''self-locating'' features in parts that would facilitate quick and error-free assembly. CAD systems and advanced machining techniques enabled designers in many cases to reduce product weight and eliminate assembly steps by using a single, complex part to replace what would otherwise be a subassembly of hundreds of parts and fasteners [5].

A special case of the above mentioned was presented in a local aerospace company in Mexicali (Baja, Mexico). The manufacturing management system required an analysis to compare an assembled component and a proposal part with the same form and material but machined in one step, where management provided information about geometry and manufacturing processes.

The assembled component location and with reference to the diagram shown in Figure 1, it has been established that the loads presented in the assembled component are the weight of turbines, pressurization and the drag force derived by propulsion force turbines. The assembled component is installed on a private plane that has two turbines that generate a thrust of 75.17kN (16,900 pounds) and weight of 21.85kN (4,912 pounds) per unit. In addition, the engine mount is provided with a mounting system inserted between the turbojet engine and the rigid structure of the engine mount, this system globally comprising at least two engine attachments, generally a forward and after attachment. The Figure 2 shows the assembly of the turbine, where similar assembled component as the one studied can be seen [6].

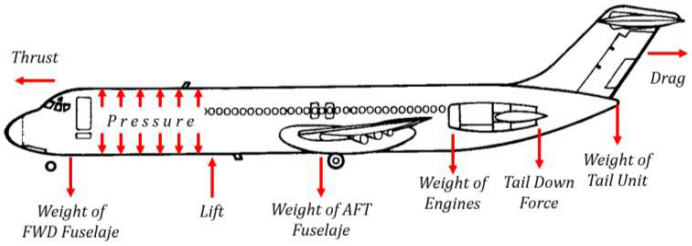


Fig. 1. Loads present in the aircraft fuselage [7].

It is considered that under the above described conditions, the drag force resulting from propulsion force turbine is the most significant for the analysis of the assembled component so thus structural elements close to installation of the turbines must have a rigid behavior.

Having said this, a non-destructive physical test was proposed, determining the embedment in the upper middle of each model because in that area a main spar is located and the application of load at each end of it, simulating the drag force caused by turbines.

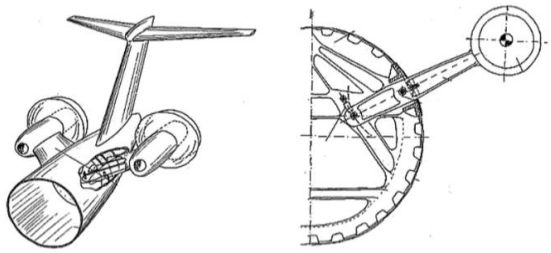

Fig. 2. Turbine assembly in aerospace structure [7].

According to the above information and the geometry of the models, it's important to add that the model was experimented a combined stress (bending-torsion). The symmetry of the models allowed to be instrumented using in each end of it a different kind of strain gage to obtain additionally the operational relationship between a single and a rectangular rosette strain gages installed in each model at these conditions.

## 2. Methodology

### *2.1. Principles*

The model of analysis is a structural aerospace assembled component located in the section of the body, closest to the tail between the engines of a private aircraft, as shown in the Figure 3 (modified by confidentiality policies). This assembled component was made of three parts with the same aluminium alloy. Two side reinforcing elements were assembled by rivets to a main part.

The manufacturing process basically consisted of the installation of the main part installation in a fixture, after the other parts were assembled each one by 46 rivets of 3.175mm (0.125in) of diameter. At the end, five holes were drilled on the body of each secondary part, of a diameter of about 12.7mm (0.5in). Based on comments of the manufacturing staff, it is a common practice to re-work the piece in the drilling phase. This process of re-work consists of making a graft material.

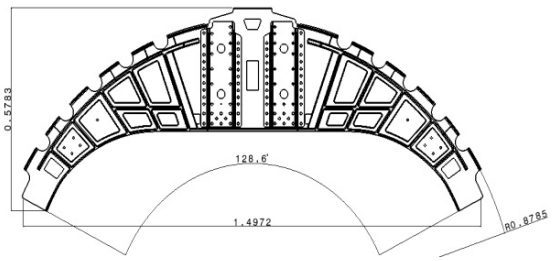


Fig. 3. Modified structural aerospace assembled component (units: meters) [7].

For the non-destructive physical test, the elements of the assembled component as the proposal part were machined using aluminium 6061 T6. The assembly process was simplified to only 2 rows with 3 rivets by part, that

is, the assembled component has 12 rivets. The used rivets were conventional of 3.175 x 6.35mm (0.125 x 2.50in). Figure 4 shows the pieces already machined.

Fig. 4. Structural aerospace assembled component as the proposal part machined in one step [7].

The Finite Element Analysis (FEA) represents a cost-effective tool in situations where precise analysis and evaluation of physical quantities (such as stress, strain, displacements, velocity, temperature, etc.) requires expensive equipment which usually may not provide outcomes for a complete structure [7].

In experimental fracture mechanics, strain gages are extensively used for measurement of various important parameters. Strain gage techniques have received much attention because of their relative ease use and measurement of surface strains accurately within the strain gradient zones [8].

Strain gages operate under the linearly elastic condition with the change of resistance ($\Delta R$) proportional to the strain ($\varepsilon$). As a strain gage undergoes stretching or compression, its electric resistance increases or decreases respectively, which we can measure using a Wheatstone bridge circuit [9].

A uniaxial (single-grid) strain gage would normally be used only when the stress state at the point of measurement is known to be uniaxial and the directions of the principal axes are known with reasonable accuracy (better than ±5°). Of course, multiple single-grid gages can be installed at desirable relative angles and spacing to solve many stress analysis problems, but most gage manufacturers supply multigrid gage on a common backing to simplify the installation process. A good example is the dual-grid pattern (rectangular rosette strain gage) where the grids are ±45° to the axis of the gage. For the most general measurement case, when the specimen stress state and principal axes are unknown, a three-element rosette should be used to determine the principal stress magnitudes and directions [10].

Having said this, a non-destructive physical test was proposed, determining the embedment in the upper middle of each model because in that area a main spar is located and the application of load at each end of it, simulating the drag force caused by turbines.

According to the above information and the geometry of the models, it's important to add that the model was experimented a combined stress (bending-torsion). The symmetry of the models allowed to be instrumented using in each end of it a different kind of strain gage to obtain additionally the operational relationship between a single and a rectangular rosette strain gages installed in each model at these conditions.

### *2.2. Materials*

The material and equipment used for the test consists of: uniaxial strain gages Omega SGT-3F/350-TY11, rectangular rosette strain gages Vishay EA-09-125RA-120, degreaser spray, conditioner, solvent, neutralizer, cell test, press type "C", test weights, Data Acquisition (or DAQ) 9174 equipment from National Instruments (NI), computer with LabVIEW, Loctite 401 glue, heat weld gun, electronic pad, tweezers, transparent tape and gauzes.

### *2.3. Methods*

Using strain gages and their connection with the DAQ-9174 equipment from NI can be obtained the strain value in one or several specific location for each model (assembled component or proposal part) in support with a

LabVIEW routine or Virtual Instrument (VI). Figure 5 shows the proposal part instrumented with uniaxial and rectangular rosette strain gages.

A DAQ based virtual instrument was designed and developed in LabVIEW programming environment. This virtual instrument has the capability to generate intelligent software trigger for complex waveforms like chirp. The main decisions during design of the virtual instrument are: choosing the data acquisition card and, what is equally important, choosing the set of features the instrument should offer. The choice of the data acquisition card has a great influence on the efficiency of the whole instrument [11].

The measurement instruments based on DAQ board connected to a common personal computer, i.e. PC-based instruments, can offer a more suitable and less expensive alternative for commercial instrumentation compared to standalone solutions. Thanks to the recent development of high-accuracy DAQ boards, it is interesting to investigate the possibility to develop high accuracy instrumentation by means of PC-based solutions [12].

LabVIEW is a graphical programming environment which helps engineers quickly to develop powerful test software with beautiful and convenient Graphical User Interface (GUI). A LabVIEW program consists of numbers of Virtual Instrument (VI). A VI consists of a front panel, a block diagram and an icon that represents the VI. The front panel displays controls and indicators for the users, while the block diagram contains the code of the VI. LabVIEW contains many basic VIs which allows the programmer to construct a GUI in a much shorter time than other conventional programming languages such as C/C++, Visual Basic, and Matlab. Its graphical nature makes it ideal for measurement and automation [13].

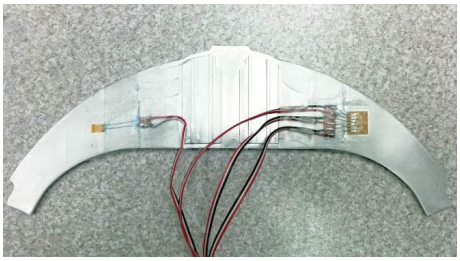

Fig. 5. Uniaxial and rectangular rosette strain gages installed in the proposal part.

## 3. Results

### *3.1. Machining of the Aerospace Parts*

In Table 1, it can observe the obtained machining time for the assembled component and the proposal part machined in one step. The findings show an evident difference of 1.83 hours, reaffirming the added benefit of converting assembled components of aluminium into a parts machined in one step.

The values show the required time for preparation (set-up) of the three-axis CNC (Computer Numerical Control), the operating times of the machine (machining) and the assembly process by conventional rivets. It is noteworthy that for the assembly part is included the drilling for placing rivets for the 3 parts.

### *3.2. Finite Element Analysis by ANSYS*

For the Analysis by ANSYS, each model is subjected to a combined stress, using the conditions described above, by the embedment in the upper middle of the model and applying different loads at each end of the model. The principal elastic strain distribution (ε) along each model is presented in Figure 6 using the maximum load value of 43.44N (10.44Lbf).

Table 1. Time required for the manufacturing process of test models [7].

| Proposal Part | | Assembled Component | |
|---|---|---|---|
| Operation | Time (hours) | Operation | Time (hours) |
| Set up | 0.28 | Main part | |
| Machined | 1.20 | Set up | 0.24 |
| Total | 1.48 | Machined | 1.11 |
| | | Secondary parts | |
| | | Set up | 0.22 (x 2) |
| | | Machined | 0.67 (x 2) |
| | | Assembly | |
| | | Riveting | 0.18 |
| | | Total | 3.31 |

In this configuration, the first rivets row near at recessed area operates as connecting and stiffening elements in the assembled component. On the other hand at the proposal part, there is a greater uniform section in which the load is distributed throughout the part.

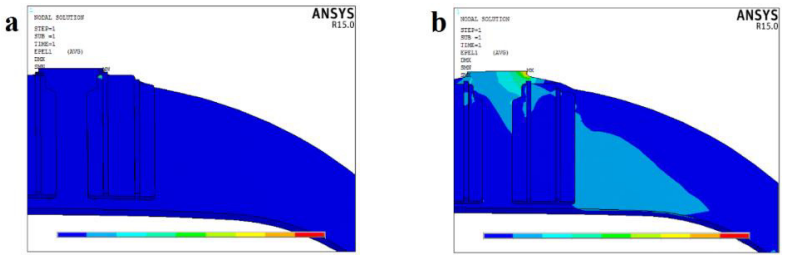


Fig. 6. Principal strain distribution at (a) Assembled Component (b) Proposal Part.

The remarkable result is located in a specific point (or node) in the two models. The node has been selected with the location of each strain gage installed at each model for making the comparative analysis. Figure 7 shows the node 4717 selected for the proposal part and the principal elastic strain value for the maximum load value. Node 2676 has been selected for the assembled component and node 4717 for the proposal part. The results obtained for each part are presented in Table 2.

By examining the obtained outcomes, it can observe the principal elastic strain difference between the two studied models, showing a significant improvement at the proposal part machined in one step, which demonstrate that this part behaves better than the assembled component.

### *3.3. Rectangular rosette strain gages*

The rectangular rosette strain gages and their connection with the NI DAQ-9174 in support with a VI, obtained the principal elastic strain value at the location of each strain gage installed at each model by applying different loads. A quarter Wheatstone bridge was used. The principal elastic strain values obtained through the NI DAQ for each model are shown in Table 2.

Table 2. Strains obtained in specific node by FEA, Rectangular rosette and uniaxial strain gage.

| Load | Assembly Component | | | Proposal Part | | |
|---|---|---|---|---|---|---|
| N | ANSYS(mε) | Rosette(mε) | Uniaxial(με) | ANSYS(mε) | Rosette(mε) | Uniaxial(με) |
| 16.10 | 0.2704 | 0.2694 | 32.363 | 0.1664 | 0.1419 | 22.310 |
| 20.01 | 0.3361 | 0.3292 | 39.513 | 0.2068 | 0.1729 | 26.880 |
| 25.88 | 0.4347 | 0.4078 | 48.838 | 0.2675 | 0.2476 | 35.940 |
| 29.80 | 0.5005 | 0.4707 | 56.263 | 0.3080 | 0.2652 | 38.530 |
| 33.71 | 0.5662 | 0.5310 | 63.338 | 0.3484 | 0.3038 | 43.250 |
| 37.63 | 0.6311 | 0.5731 | 68.213 | 0.3884 | 0.3386 | 47.630 |
| 42.52 | 0.7140 | 0.6419 | 76.319 | 0.4394 | 0.3682 | 51.100 |
| 46.44 | 0.7793 | 0.7012 | 83.313 | 0.4796 | 0.5156 | 65.320 |

These results are consistent with the trend of the analysis with ANSYS; the proposal part machined in one step has a lower strain compared to the assembled component.

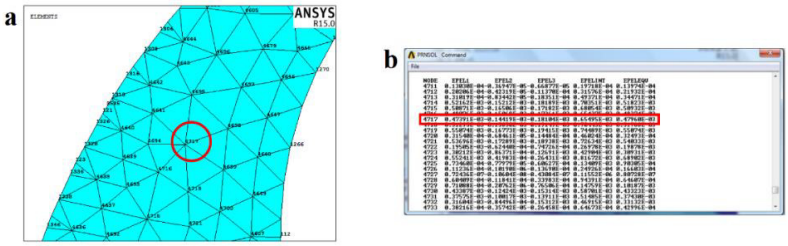


Fig. 7. (a) Node 4717 at proposal part model (b) Principal elastic strain value screen in ANSYS.

### *3.4. Uniaxial strain gages*

The uniaxial strain gages obtained an elastic strain component at the location of each strain gage installed at each model by applying different loads. This component represents the elastic strain obtained by bending stress due to the uniaxial strain gage orientation. A quarter Wheatstone bridge was used. The component elastic strains values for each model are shown in Table 2. These findings are coherent with the trend of previous analyses; the proposal part machined in one step has a lower strain compared to the assembled component.

## 4. Conclusions

The results show that the proposal part machined in one step has a trend to obtain less strain (0.5156mε@46.44N) with rectangular rosette strain gage; 0.4796 with FEA) than the assembled component, (0.7012mε@46.44N with rectangular rosette strain gage; 0.7793 with FEA). These outcomes indicate that the proposal part works better in this operating condition, therefore to be a structural element with greater structural stiffness in comparison to the assembled component. These findings suggest that the arrangement used for the test has a satisfactory geometric shape, since only the first rivets row near at the embedding area act as connecting and stiffening elements in the assembled component and, the proposal part has a greater section in which load is distributed uniformly along the model. Therefore, it may indicate that the proposal part has achieved an improvement in stiffness and structural stability under the actual operation. We also consider that is important to establish the condition of structural improvement based on the desired behavior, because on this particular case, based on the location of the component in the plane's fuselage, structural stiffness is required for transmission effort through the stringers and bulkheads, goal achieved by the conversion.Although the results in both strain gages (rectangular rosette and uniaxial) shown a

beneficent trend to the proposal part concerning to the assembled component, exists a considerable difference between the obtained outcomes. The difference is because the rectangular rosette strain gage obtained the principal elastic strain value per the combined stress (bending-torsion) and the uniaxial strain gage obtained an elastic strain component that is equivalent to the strain induced by bending stress due to the uniaxial strain gage orientation. These results suggest that even if showed the mentioned trend, could be inaccurate take the uniaxial strain gage measures as a decision factor in order to determinate a conversion of that kind, because the rectangular rosette strain gage measures proposed that torsion stress is predominant by the operational conditions described above. Discussing the ANSYS findings is noteworthy that these can only be compared with the outcomes obtained from the rectangular rosette strain gage because both represent the principal elastic strain value. The uniaxial strain gage results indicate only a component that represents the elastic strain obtained by bending stress due to the strain gage (comparing results between ANSYS and the uniaxial strain gage would be wrong). Comparing the results obtained by ANSYS and the rectangular rosette strain gage (as shown Table 2), it's evident the precision between both findings. The dispersion in the findings is more evident with the proposal part. However, the instrumentation using a rectangular rosette strain gage remains as a viable method to recognize the structural stiffness of components with different applications. Regarding the reduction of time in the production and manufacturing processes, the results reaffirming the added benefit of converting aluminium parts assembled into unitary parts. The estimation of the cost savings is difficult to obtain because of the limitations on confidentiality policies Aerospace Company, from where the piece was taken for study.

## Acknowledgements

Authors express their gratitude to the Mexican National Council for Science and Technology (CONACYT) for the scholarship for Ismael Mendoza Muñoz (CVU 404945) to pursue the postgraduate studies, in where part of this work was made. Authors appreciate to the Autonomous University of Baja California (UABC) for facilitating access and use of its facilities and equipment to carry out the experimental part.

## References

[1] H.A. ElMaraghy, T. AlGeddawy. Co-evolution of Products and Manufacturing Capabilities and Application in Automotive Assembly. Flexible Services and Manufacturing Journal. Volume 24, Issue 2, (2012), pp. 142–170.

[2] A.S.M. Hoque, P.K. Halder, M.S. Parvez, T. Szecsi. Integrated manufacturing features and Design-for-manufacture guidelines for reducing product cost under CAD/CAM environment. Computers & Industrial Engineering Journal, Volume 66, Issue 4, (2013), pp. 988-1003.

[3] K.L. Edwards. Towards more strategic product design for manufacture and assembly: priorities for concurrent engineering. Materials & Design Journal, Volume 23, Issue 7, (2002), pp. 651-656.

[4] E. Tempelman, H. Shercliff, B. Ninaber van Eyben. Chapter 12 - Joining and Assembly. Manufacturing and Design Journal, (2014), pp. 201-226.

[5] T.R. Browning, R.D. Heath. Reconceptualizing the effects of lean on production costs with evidence from the F-22 program. Journal of Operations Management, Volume 27, Issue 1, (2009), pp. 23-44.

[6] I. Mendoza-Munoz, V. Nuno-Moreno, A. Gonzalez-Angeles, S.V. Medina-Leon. Comparative Analysis of a Structural Aerospace Assembly Part and an Unitary Machined Part Using Uniaxial Strain Gage and FEA. Journal of Applied Sciences, Volume 15, Issue 1, (2015), pp. 146-152.

[7] A.M. Vukicevic, L.U. Velicki, G.R. Jovicic, N.Jovicic, M.M. Stojadinovic, N.D. Filipovic. Finite element analysis of uncommonly large renal arteriovenous malformation - Adjacent renal cyst complex. Journal of Computers in Biology and Medicine, Volume 59, Issue 1, (2015), pp. 35-41.

[8] H. Sarangi, K.S.R.K. Murthy, D. Chakraborty. Optimum strain gage location for evaluating stress intensity factors in single and double ended cracked configurations. Journal of Engineering Fracture Mechanics, Volume 77, Issue 16, (2010), pp. 3190–3203.

[9] Huai-Ti Lin, B.A. Trimmer. A new bi-axial cantilever beam design for biomechanics force measurements. Journal of Biomechanics, Volume 45, Issue 13, (2012), pp. 2310–2314.

[10] W. N. Sharpe. Springer Handbook of Experimental Solid Mechanics. Springer Science & Business Media, United States, (2008), pp. 311.

[11] K.P.S. Rana, S.H. Khan. A DAQ card based mixed signal virtual oscilloscope. Journal of Measurement, Volume 41, Issue 9, (2008), pp. 1032-1039.

[12] A. Cataliotti, V. Cosentino, A. Lipari, S. Nuccio, D. Serazio. DAQs-based wattmeters for high accuracy measurements. Comparison with the Italian power primary standard. Journal of Measurement, Volume 46, Issue 9, (2013), pp. 3460–3468.

[13] Z. Wang, Y. Shang, J. Liu, X. Wu. A LabVIEW based automatic test system for sieving chips. Journal of Measurement, Volume 46, Issue 1, (2013), pp. 402–410.